

Chapter 1

Controlling Chimera Patterns in Networks: Interplay of Structure, Noise, and Delay

Anna Zakharova, Sarah A.M. Loos, Julien Siebert,
Aleksandar Gjurchinovski, Jens Christian Claussen and
Eckehard Schöll

Abstract We investigate partially coherent and partially incoherent patterns (chimera states) in networks of Stuart-Landau oscillators with symmetry-breaking coupling. In particular, we study two types of chimera states, amplitude chimeras and chimera death, under the influence of time delay and noise. We find that amplitude chimeras are long-living transients, whose lifetime can be controlled by varying the noise intensity and the value of time delay.

1.1 Introduction

Collective behavior of coupled nonlinear dynamical systems can take diverse forms, ranging from various synchronization patterns and oscillation suppression to chimera states, which have been receiving growing interest of researchers from different fields during the past decade [1]. Originally found for the model of phase oscillators [2, 3], chimera states imply spatial coexistence of coherent (synchronized) and incoherent (desynchronized) domains in a dynamical network and have been found in a large variety of different systems [4–29]. The most intriguing feature of chimera states is that they appear for networks of identical elements and symmetric coupling configurations.

Numerous experimental reports on chimera states [30–40] have stimulated further investigations in the field. Additionally, the burst of activity in chimera research is motivated by the wide range of its possible applications. In neural networks, for

A. Zakharova (✉) · S.A.M. Loos · J. Siebert · E. Schöll
Institut für Theoretische Physik, Technische Universität Berlin, Hardenbergstr. 36, 10623 Berlin,
Germany
e-mail: anna.zakharova@tu-berlin.de

A. Gjurchinovski
Institute of Physics, Faculty of Natural Sciences and Mathematics,
Sts. Cyril and Methodius University, P. O. Box 162, 1000 Skopje, Macedonia

J.C. Claussen
Computational Systems Biology Lab, Jacobs University Bremen, Campus Ring 1, 28759 Bremen,
Germany

example, chimeras can be associated with bump states [41] and in the dynamics of the heart they may be used to model ventricular fibrillation [42]. In the investigation of power grids it is important to understand how to avoid chimera states, since they may initiate a blackout—partial or full desynchronization of the power network [43]. For social systems chimeras may be linked to the situation of partial consensus in the two-population network of social agents [44]. Unihemispheric sleep of some sea mammals and birds can be related to chimera behavior [45]. Chimeras have also been suggested as a mechanism for the termination of epileptic seizure [46].

In recent studies chimera states have been extended to systems which involve not only phase but also amplitude dynamics and named amplitude-mediated chimeras in the case when both amplitude and phase are characterized by chimera behavior [20, 21]. More complicated patterns in which chimera structures are formed with respect to the amplitudes while the phases remain correlated for the whole network have been first reported in [47]. This particular type of chimera states, *amplitude chimeras*, is investigated in the present work.

While modelling real-world systems it is important to take stochasticity and time delay into account. Arising naturally, these two factors lead to a plethora of complex phenomena with applications to various fields. Moreover, both may result in opposite effects and can be exploited for control purposes. Our objective is to establish efficient control mechanisms based on noise and time delay. In particular, we address the question of how time delay and noise influence the behavior of amplitude chimera states in networks of Stuart-Landau oscillators. Additionally, we study another recently discovered type of chimera states, *chimera death* [47], which, through death of the oscillations, generalizes the chimera feature of coexistence of spatially coherent and incoherent domains to steady states.

1.2 Model

We consider a network of N Stuart-Landau oscillators [2, 47–50] under the impact of external white noise $\xi_j(t)$ and in the presence of time delay τ . The local deterministic dynamics of each node $j \in \{1, \dots, N\}$ is given by $\dot{z}_j = f(z_j)$, with the normal form of a supercritical Hopf bifurcation

$$f(z_j) = (\lambda + i\omega - |z_j|^2)z_j, \quad (1.1)$$

where $z_j = x_j + iy_j = r_j e^{i\phi_j} \in \mathbb{C}$, with $x_j, y_j, r_j, \phi_j \in \mathbb{R}$, and $\lambda, \omega > 0$. At $\lambda = 0$ a Hopf bifurcation occurs, so that for $\lambda > 0$ the single Stuart-Landau oscillator exhibits self-sustained oscillations with frequency ω and radius $r_j = \sqrt{\lambda}$, and the unique fixed point $x_j = 0, y_j = 0$ is unstable.

We investigate a ring of N non-locally coupled Stuart-Landau oscillators, where each node is coupled to its P nearest neighbors in both directions with the strength $\sigma > 0$, and is subject to noise of intensity $D > 0$:

$$\dot{z}_j = f(z_j) + \frac{\sigma}{2P} \sum_{k=j-P}^{j+P} (\text{Re}z_k - \text{Re}z_j) + \sqrt{2D}\xi_j(t) \quad (1.2)$$

where $j = 1, 2, \dots, N$ and all indices are modulo N . The normalized number of nearest neighbors P/N is denoted as coupling range. The coupling and the noise are only applied to the real parts, and $\xi_j(t) \in \mathbb{R}$ is additive Gaussian white noise [51], i.e., $\langle \xi_j(t) \rangle = 0$, $\forall j$, and $\langle \xi_i(t)\xi_j(t') \rangle = \delta_{ij}\delta(t-t')$, $\forall i, j$, where δ_{ij} denotes the Kronecker-Delta and $\delta(t-t')$ denotes the Delta-distribution. Hence the noise is spatially uncorrelated.

Further we study the impact of time delay using the following model:

$$\dot{z}_j = f(z_j) + \frac{\sigma}{2P} \sum_{k=j-P}^{j+P} (\text{Re}z_k(t-\tau) - \text{Re}z_j(t)), \quad (1.3)$$

where τ is time delay.

1.3 Deterministic Amplitude Chimera and Chimera Death

For a deterministic network with instantaneous coupling as demonstrated in [47], various different states can be found in the network given by Eq. (1.2). Which particular state actually arises, depends on the specific values of the coupling parameters and the initial conditions, as Eq. (1.2) describes a multistable system. Among the possible states, two different types of asymptotically stable states can be found, on the one hand oscillatory states, and on the other hand steady state patterns which are related to oscillation death. The latter are represented by completely coherent or completely incoherent oscillation death patterns, as well as by chimera death patterns consisting of coexisting domains of coherent and incoherent steady states. The asymptotically stable oscillatory states appear in two different spatio-temporal patterns: in-phase synchronized oscillations and coherent traveling waves. Besides these, long lasting oscillatory transients with interesting features occur, i.e., amplitude chimera states. In this work we demonstrate that all these states can also be observed under the influence of noise and time delay. Before an asymptotic oscillatory state is approached, *amplitude chimera* states can appear as long transients, potentially lasting for hundreds or even thousands of oscillation periods. In contrast to classical phase chimeras, all nodes (including the ones within the incoherent domains) oscillate with the same period, $T = \frac{2\pi}{\omega}$, and a spatially correlated phase, but they show spatially incoherent behavior with respect to the *amplitudes* in part of the system. Figure 1.1 shows an exemplary amplitude chimera configuration. The nodes within the two coherent domains (here $13 \leq j \leq 85$ and $113 \leq j \leq 185$) perform synchronized oscillations, all with the same amplitudes. The coherent domains always appear pairwise, such that for every time t , all nodes within one coherent domain have a phase lag of π with

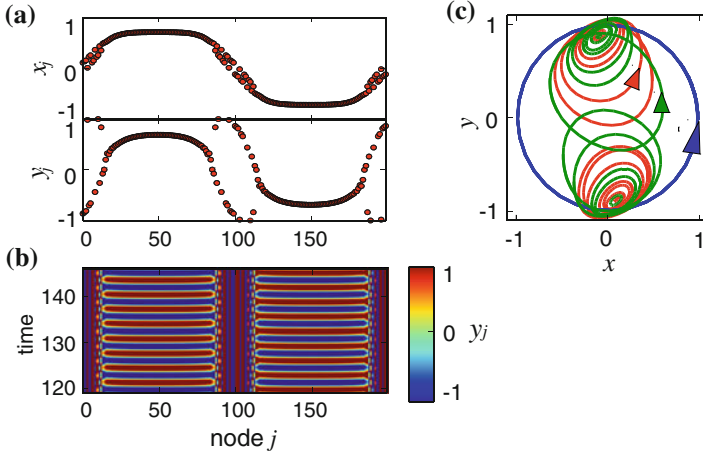


Fig. 1.1 Amplitude chimera state in system (1.2) with $N = 200$ nodes, for coupling range $P/N = 0.04$ and coupling strength $\sigma = 18$: **a** snapshot (top x_j , bottom y_j), **b** space-time plot, **c** phase plot in the complex plane: trajectories of 12 nodes of the incoherent (red and green), and 12 nodes of the coherent (blue) domains, the arrows indicate the direction of the motion. Initial condition: See Sect. 1.4. Other parameters: $D = 0$, $\lambda = 1$, $\omega = 2$

respect to all nodes of the other, antipodal domain. Hence they always fulfill the “anti-phase partner” condition $z_j = -z_{j+N/2}$, $j \bmod N$, assuming even N . As visible in Fig. 1.1c, the trajectories in the complex plane of all nodes are cycles, illustrating that all nodes have periodic dynamics in time. This is a fundamental difference between the classical phase chimera states where a part of the network demonstrates chaotic temporal behavior. The nodes of the coherent domains all oscillate on a perfect circle around the origin. Both coherent domains are represented by one single blue line in Fig. 1.1c, which as well represents time the trajectory of all nodes when the completely in-phase synchronized oscillatory solution is approached. The two antipodal coherent domains are separated by incoherent domains. There, neighboring nodes can be in completely different states at a given time t . Their trajectories are deformed circles, whose centers are shifted from the origin. The *completely arbitrary sequence* of nodes that oscillate around centers in the upper and in the lower half-plane reflects the incoherent nature. Transient amplitude chimeras with very narrow incoherent domains can be observed, as well as with broad ones.

If the coupling strength and coupling range exceeds certain values, the oscillations of the Stuart-Landau nodes can be suppressed due to the stabilization of a new inhomogeneous steady state created by the coupling. Instead of performing oscillations, each node approaches a fixed point close to one of the following two branches: $(x^{*1}, y^{*1}) \approx (-0.1, +0.85)$ or $(x^{*2}, y^{*2}) \approx (+0.1, -0.85)$ (for $\lambda = 1$), and remains there for all times. The oscillation death states exhibit a huge variety of spatial patterns, including multiple coherent and multiple incoherent oscillation death states [47, 50, 52, 53]. Two exemplary configurations of completely coherent oscilla-

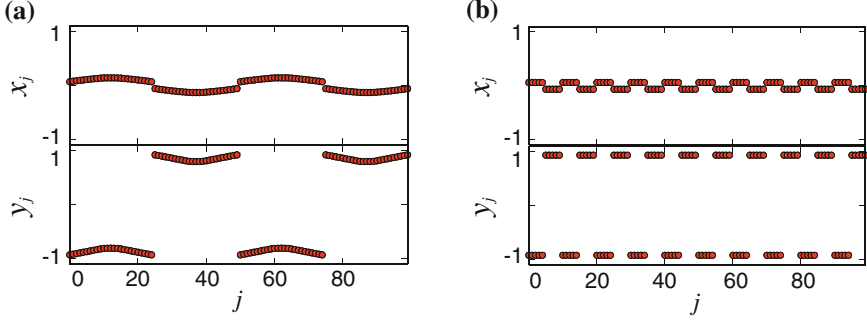


Fig. 1.2 Snapshots of coherent oscillation death states: **a** coupling strength $\sigma = 18$ and coupling range $P/N = 0.14$ (2-cluster), **b** $\sigma = 8$, $P/N = 0.04$ (10-cluster). *Initial condition:* Nodes $0 \leq j \leq 24$ and $50 \leq j \leq 74$ are set to $(x_j, y_j) = (0.1, -1)$, all other nodes are set to $(x_j, y_j) = (-0.1, +1)$. *Other parameters:* $N = 100$, $D = 0$, $\lambda = 1$, $\omega = 2$

tion death patterns are shown in Fig. 1.2 (2-cluster and 10-cluster oscillation death). The oscillation death regime is characterized by very high multistability. Among the oscillation death states, *chimera death* patterns can be found, which combine the characteristics of both phenomena: chimera state and oscillation death. These patterns consist of coexisting domains of coherent and incoherent populations of the inhomogeneous steady state branches. Within the incoherent domains, the population of the two branches (upper and lower) follows a random sequence, as for example visible in Fig. 1.3. Within the coherent domains, the number of clusters of neighboring nodes that populate the same branch of the inhomogeneous steady state can vary. An m -cluster chimera death state (m -CD), with $m \in \{1, 3, 5, 7, 9, \dots\}$, is characterized by the occurrence of m clusters i.e., sets of neighboring nodes that populate the same branch of the inhomogeneous steady state within each coherent domain. The coherent domains always appear pairwise with anti-phase symmetry $z_j = -z_{j+N/2}$, similarly to the coherent domains of the amplitude chimera configurations. Our numerical results confirm that the stable oscillation death patterns fulfill the “anti-phase partner” condition.

1.4 The Impact of Initial Conditions

For $D = 0$, Eq. (1.2) is known to describe a multistable system [47]. Both types of chimera states appear in coupling parameter regimes, where other oscillation death patterns and coherent oscillatory states can be found as well. In order to increase the probability of finding chimera states, we use specially prepared initial conditions [54]. A very simple initial condition that produces transient amplitude chimeras in a certain parameter regime (of about $0.01 < P/N < 0.05$, $\sigma < 33$), is when all nodes of one half of the network ($1 \leq j \leq \frac{N}{2}$) are set to the same value $(x_j, y_j) = (x_0^1, y_0^1)$

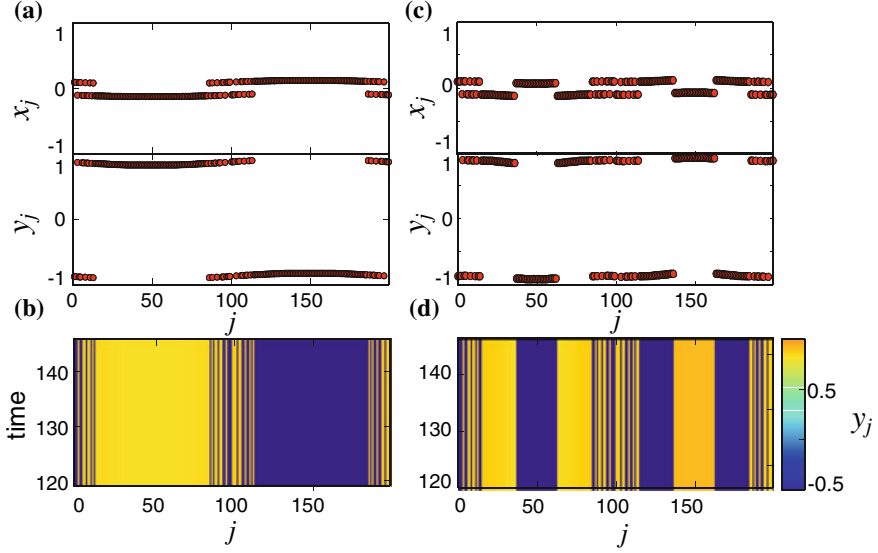


Fig. 1.3 **a, b** 1-cluster chimera death (1-CD) for coupling range $P/N = 0.4$, **c, d** 3-cluster chimera death (3-CD) for $P/N = 0.2$. Snapshots x_j, y_j are shown in panels (a, c), space-time plots in panels (b, d). *Initial condition:* See Sect. 1.4. *Parameters:* $N = 200, \sigma = 18, D = 0, \lambda = 1, \omega = 2$

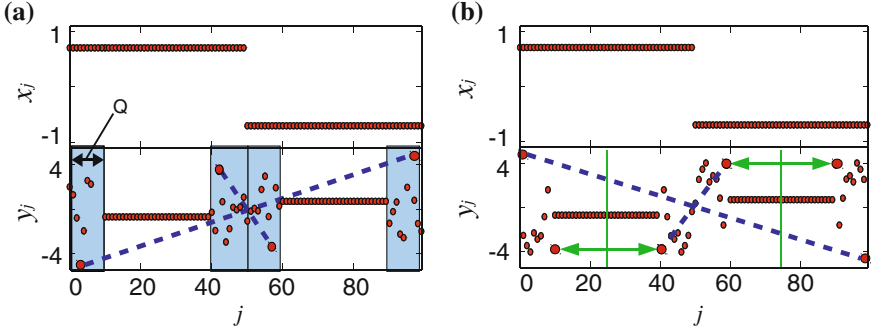


Fig. 1.4 Specially prepared initial conditions for amplitude chimeras: **a** point-symmetric type, **b** fully-symmetric type. *Top panels* x_j , *bottom panels* y_j . *Dashed lines* indicate the point-symmetry about the center, *solid green lines* indicate the axial symmetry within both network halves. *System size* $N = 100$

(excluding the choice $(0, 0)$), and the rest is set to $(x_0^2, y_0^2) = (-x_0^1, -y_0^1)$. Hence, amplitude chimera states can evolve out of initial configurations that only consist of two completely coherent parts. We choose the values $(x_0^1, y_0^1) = (\sqrt{0.5}, -\sqrt{0.5})$, so that the nodes start on the limit cycle with $r = \sqrt{\lambda} = 1$, which is the solution for the in-phase synchronized oscillation. The amplitude chimera lifetime nevertheless appears to be of the same order for other values (e.g. $(x_0^1, y_0^1) = (1, -1)$).

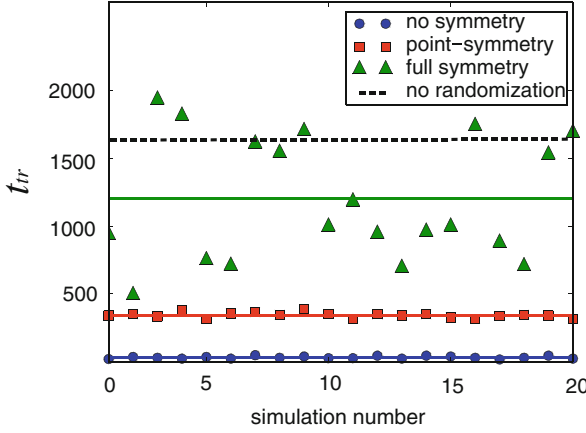


Fig. 1.5 Transient times of amplitude chimera states t_{tr} for 20 realizations of specially prepared random initial conditions (no symmetry, point-symmetry, full symmetry, depicted by different symbols) with $Q = 10$, $V = 2$. Horizontal solid lines Mean values. Dashed line t_{tr} for the initial condition with $V = 0$ (no randomization). System parameters $N = 100$, $\sigma = 14$, $P/N = 0.04$, $D = 0$, $\lambda = 1$, $\omega = 2$

By adding random numbers to y_j , we construct a more general class of specially prepared random initial conditions for amplitude chimeras. In particular, we add a random number drawn from a Gaussian distribution with variance V to y_j of the Q nodes on the left and on the right side of the borders between both halves (at $j = \frac{N}{2}$ and $j = N$), as indicated in Fig. 1.4a, with $Q \in \mathbb{N}$ and $0 < Q \leq \frac{N}{4}$. Besides the range Q of incoherence, we also vary $V \geq 0$. For a proper choice of the two initial condition parameters (Q and V), we obtain amplitude chimeras. Using the achieved amplitude chimera lifetime as a quality measure for the initial condition, we compare multiple realizations of the specially prepared random initial conditions for the deterministic system with $P/N = 0.04$ and $N = 100$. We observe that among all considered kinds of initial conditions (different choices for Q and V , symmetry conditions, x_j randomized as well, a different underlying distribution for the random numbers), the applied symmetry of the initial condition has the greatest effect upon the transient time.

Figure 1.5 shows the transient times and their mean value (solid lines) for multiple realizations of the initial conditions following three different symmetry schemes. For the particular choice ($Q = 10$, $V = 2$) all symmetry types lead on average to shorter lifetimes than an initial condition without random component (black dashed line). For the initial configurations without symmetry, a random number is chosen independently for each node within the four incoherent intervals. These configurations clearly create the shortest amplitude chimera lifetimes, lasting at most for a couple of oscillation periods. This symmetry type also leads to the shortest transients in other regimes of Q , and V (not shown here). In contrast, for the point-symmetric initial conditions, we mirror the random numbers used for $j \in \{1, \dots, \frac{N}{2}\}$ with respect to the center $j = 0$, $y_j = 0$, and use their negative counterparts for the second half.

We hence only generate $2Q$ random numbers in total. The initial configurations are point-symmetric with respect to the center, see Fig. 1.4a. The lifetimes of the occurring amplitude chimeras are much longer than in the non-symmetric case. However, the symmetry type which leads to the longest lifetimes is the one referred to as full symmetry; the initial conditions fulfill two symmetries: The randomly chosen values of the positions of the nodes within the first incoherent interval $1 \leq j \leq Q$ are mirrored to the nodes $\frac{N}{2} - Q \leq j \leq \frac{N}{2}$, by setting: $z_j = z_{\frac{N}{2}+1-j}$. To obtain the positions of the second network half, then a phase shift of π is applied, such that the “anti-phase partner” condition is fulfilled ($z_j = -z_{j+\frac{N}{2}}$ and $j \bmod N$). Thus, we only generate Q different random numbers in total. The configurations are again point-symmetric with respect to the center, and have an additional axial symmetry with orthogonal axes through $j = \frac{N}{4}$ and $j = \frac{3N}{4}$, as indicated in Fig. 1.4b. Of course, the simple initial condition with no randomization also fulfills these symmetry conditions and can therefore be regarded as one special type of the fully-symmetric specially prepared initial conditions (with $V = 0$). We have further tested another type of initial condition that solely fulfills the anti-phase partner condition: $z_j = -z_{j+\frac{N}{2}}$, but has no other symmetries. This type of initial condition also certainly leads to transient amplitude chimeras, but only within very narrow ranges of Q and V . For $Q = 10$, $V = 2$, the mean lifetime (of about $t_{tr} \approx 49$) is only slightly increased compared to the non-symmetric initial condition (not shown here). Since the symmetry which is applied to the initial conditions remains preserved during the dynamic evolution, this observation means that the fully-symmetric amplitude chimeras are most stable and have the longest lifetimes.

By decreasing the variance in the interval $0.1 \leq V \leq 2$, the mean amplitude chimera lifetimes increase. In the range of small variances of about $V < 0.5$, amplitude chimeras occur for all choices of the incoherence range Q , and the particular choice of Q does not influence the transient time much. For $Q = \frac{N}{4}$, all nodes are randomized, see Fig. 1.6a, which appears to be a natural choice. Figure 1.6b shows the corresponding transient times belonging to a set of 40 realizations of the specially prepared random initial condition with $Q = \frac{N}{4}$ and $V = 0.5$, and for a set with $V = 0.1$. The mean transient times are much longer than for $V = 2$ (cf. Fig. 1.5). They are at least of the same order (and can be larger) as the transient time for the simple initial condition with no randomization, $V = 0$ (dashed black line). For the choice $V = 0.1$, the transient times are increased as compared to $V = 0.5$. We use the fully-symmetric initial conditions with $Q = \frac{N}{4}$ and $V = 0.1$ for all investigations presented in this chapter.

Besides oscillatory states, oscillation death states can occur in a large variety of different spatial patterns. Our numerical results suggest that in the appropriate parameter regime every amplitude chimera snapshot can be used as initial condition to certainly produce a chimera death state. How many clusters in the coherent domain of the chimera death pattern occur, depends on the initial condition as well as on the parameter choice (see Sect. 1.5.2).

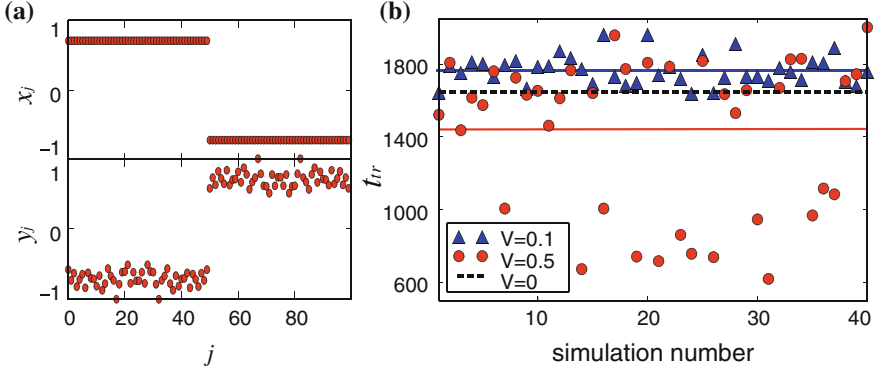


Fig. 1.6 **a** Fully-symmetric random initial condition with range of incoherence $Q = \frac{N}{4}$ and variance $V = 0.1$. **b** Transient times of amplitude chimeras t_{tr} for 40 realizations of the initial condition shown in **(a)**: circles $V = 0.5$, triangles $V = 0.1$. Horizontal solid lines: Mean values, dashed line: t_{tr} for $V = 0$. System parameters: $N = 100$, $\sigma = 14$, $P/N = 0.04$, $D = 0$, $\lambda = 1$, $\omega = 2$

1.5 Stochastic Case

1.5.1 Control of Amplitude Chimera Lifetime by Noise

In this section we will study the role of noise for chimera patterns [54]. By using the same initial conditions which lead to amplitude chimera states and chimera death in the deterministic case, we also observe these states in Eq. (1.2) in the presence of noise in a wide range of the coupling parameters. Figure 1.7 shows one exemplary configuration for an amplitude chimera which occurs in a system under the impact of noise of intensity $D = 5 \cdot 10^{-3}$.

In general, the transient times of amplitude chimeras decrease with increasing noise intensity. Figure 1.8 shows the average transient times and the corresponding standard deviations in dependence of the noise intensity D , for three choices of the coupling strength σ , in a semi-logarithmic plot. The average is over 50 different fully symmetric initial conditions (with $Q = \frac{N}{4}$, see Sect. 1.4) drawn from different realizations of the associated random distribution. For each one of those realizations of the initial conditions, a different realization of the Gaussian white noise $\xi_j(t)$ is considered. The average transient times show a clear linear decrease as a function of the logarithmic noise intensity. This behavior is found throughout the range $6 \leq \sigma \leq 24$, i.e., $t_{tr} = -\frac{1}{\mu} \ln(D) + \eta$ with slope $-\frac{1}{\mu}$ and axis intercept η . This gives the scaling law

$$D \sim e^{-\mu t_{tr}}. \quad (1.4)$$

The lines in Fig. 1.8 show the linear fits, and the inset depicts the slope in dependence on the coupling strength σ . For the same set of 50 initial conditions, Fig. 1.9a depicts the mean transient time in dependence of the coupling strength for four different

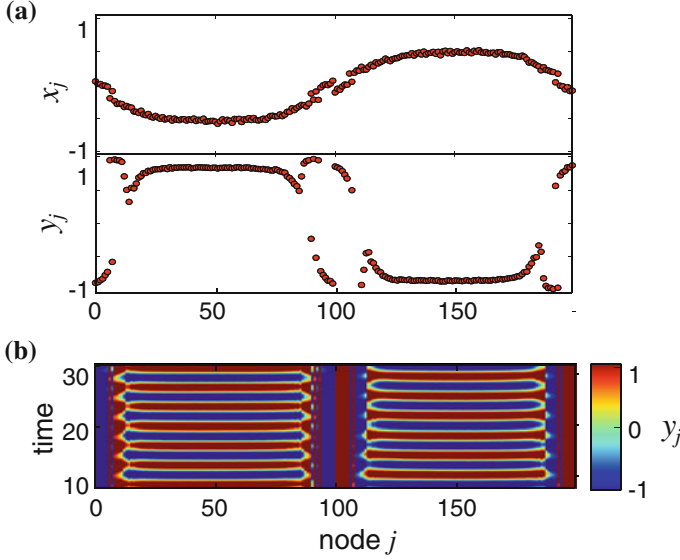


Fig. 1.7 Amplitude chimera for noise intensity $D = 5 \cdot 10^{-3}$: **a** snapshot (top x_j , bottom y_j), **b** space-time plot. Parameters: $N = 200$, $P/N = 0.04$, $\sigma = 19$, $\lambda = 1$, $\omega = 2$. Initial condition: See Sect. 1.4

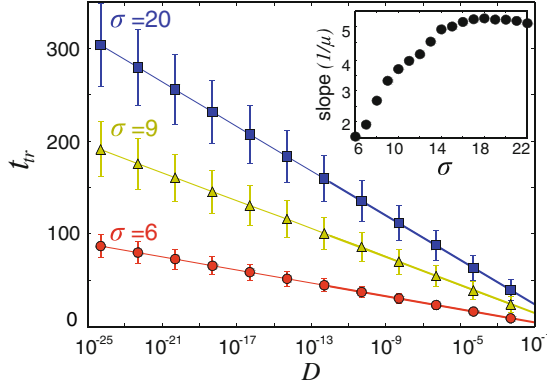


Fig. 1.8 Transient times of amplitude chimeras t_{tr} versus noise strength D (log-scaled) for different values of coupling strength σ . Symbols: Average over 50 fully symmetric initial conditions (with $Q = \frac{N}{4}$), each associated with a different realization of the random force $\xi(t)$; error bars: standard deviations; lines: linear fits from Eq.(1.4). Inset: Slope versus σ . Parameters: $N = 100$, $P/N = 0.04$, $\lambda = 1$, $\omega = 2$

noise intensities D , and Fig. 1.9b shows a color-coded density plot of the mean transient times of amplitude chimeras in the (σ, D) -plane. The transient times generally decrease with increasing noise, and increase with increasing coupling strength up to a saturation value at about $\sigma \approx 15$. The vertical error bars in panel (a) show that

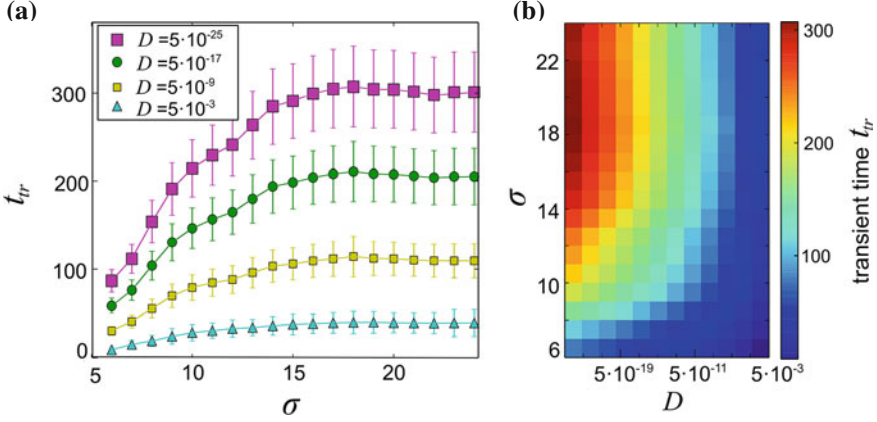
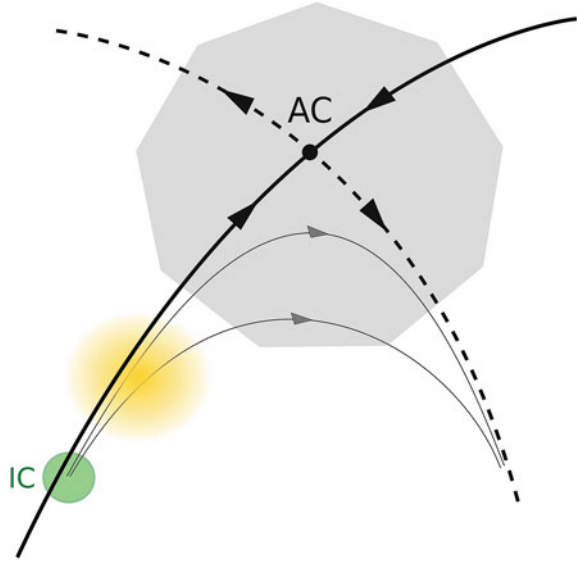


Fig. 1.9 Transient times of amplitude chimeras t_{tr} averaged over 50 initial conditions and noise realizations (the same set of initial conditions as used in Fig. 1.8): **a** t_{tr} versus coupling strength σ for different noise intensities. *Symbols*: Mean transient times; *error bars*: standard deviations. The *lines* serve as a guide to the eye. **b** t_{tr} in the plane of coupling strength σ and noise intensity D . *Other parameters*: $N = 100$, $P/N = 0.04$, $\lambda = 1$, $\omega = 2$

the transient times are less sensitive to the initial condition, the larger the noise is. We generally find that the spread of the amplitude chimera lifetimes for different initial conditions (and different noise realizations), is smaller with increasing noise strength.

Transient amplitude chimeras can last for thousands of oscillation periods until they disappear. Even under disturbance by external noise they persist for a significant time. Noise does not essentially change their spatial configuration. If noise throws the system onto an adjacent trajectory in the underlying high-dimensional phase space of the network, this does not normally lead to a flow into a completely different direction in phase space. Geometrically speaking, this shows that there are some attracting directions in phase space along which the system dynamics is pushed towards the amplitude chimera. Furthermore, amplitude chimeras can evolve out of initial configurations that do not show the characteristic coexistence of coherent and incoherent domains (see Sect. 1.4). In fact, they can be observed when completely incoherent initial configurations are used, as well as when the initial condition consists of two completely coherent parts. These dynamical properties indicate that the flow within a certain volume of the phase space is directed towards the amplitude chimera state. From the perspective of the amplitude chimera, there must exist some associated “stable directions”. However, even in the absence of any external perturbation, for all system sizes, the amplitude chimera states disappear after some time, and the system approaches a coherent oscillatory state. Accordingly, there must also exist at least one “unstable direction” in phase space. These findings can be explained by the structure of the phase space, which is schematically depicted in Fig. 1.10.

Fig. 1.10 Schematic phase-space structure of an amplitude chimera (AC) as a saddle-point. *Thick solid lines*: Stable directions, *thick dashed lines*: unstable directions, *thin solid lines*: different trajectories, with arrows denoting the direction of time evolution. *Grey shaded region*: Scheme of amplitude chimera configuration, *green disk*: set of initial conditions (IC), *yellow area*: impact of Gaussian white noise



The lifetime of amplitude chimeras in the deterministic case strongly depends on the choice of initial conditions as discussed in Sect. 1.4. In general the sensitivity of chimera states to the initial configurations is explained by the fact that classical chimera states typically coexist with the completely synchronized state, for which the basin of attraction is significantly larger. For amplitude chimeras, all our numerical results support the idea that amplitude chimera patterns can be seen as a saddle state composed of stable (solid lines in Fig. 1.10) and unstable (dashed lines Fig. 1.10) manifolds. The set of initial conditions leading to amplitude chimeras can be represented as a volume restricted in phase space (green disk in Fig. 1.10). The observed amplitude chimera corresponds to trajectories starting from this set and passing the saddle-point from the stable direction towards the unstable manifold. The lifetime of an amplitude chimera, therefore, depends on the chosen trajectory: the closer to the saddle-point it gets, the longer is the lifetime. In other words, the transient time is determined by the time the system spends in the vicinity of the saddle-point where coherent and incoherent oscillating domains coexist before it escapes to the in-phase synchronized regime along the direction of the unstable manifold. Such a phase space scenario explains the sensitivity of transient times to initial conditions since they determine the particular path the system takes.

Our numerical investigations of the stochastic model Eq. (1.2) show that Gaussian white noise dramatically reduces the impact of initial conditions on the lifetime of amplitude chimeras. In more detail, we have tested a set of realizations of initial conditions which lead to significantly different lifetimes of amplitude chimeras without random forcing. In the presence of relatively weak noise $D = 5 \cdot 10^{-13}$ all realizations result in amplitude chimeras with similar lifetime. This again supports our view of the amplitude chimera as a saddle-point, and allows for the following explanation.

The stochastic force, which continuously perturbs the system, makes it randomly switch between different trajectories close to the saddle-point. Therefore, the system's dynamics is not determined by a single trajectory anymore, but rather affected by a set of trajectories belonging to the N -dimensional hyper-sphere. This reduces the sensitivity of the amplitude chimera lifetime to specific initial conditions. In Fig. 1.10 the impact of noise is illustrated by yellow shading, denoting the stochastic forces applied to the system at one instant of time.

1.5.2 Maps of Dynamic Regimes: Interplay of Noise and Coupling

For a large range of the coupling parameters σ and P we calculate the asymptotically stable state and the transient time of amplitude chimeras for $N = 100$. For each choice of (σ, P) we start with the same amplitude chimera configuration as initial condition. For an exemplary initial condition, the results belonging to four different noise intensities are shown in Fig. 1.11. For very small coupling strength σ or very small coupling range P/N the asymptotic states are coherent oscillatory

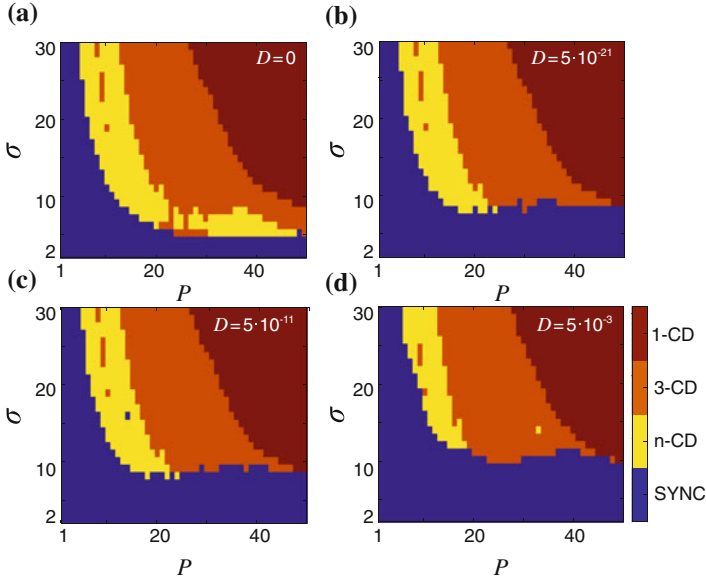


Fig. 1.11 Map of dynamic regimes in the plane of coupling strength σ and number of nearest neighbors P for noise intensities: **a** $D = 0$, **b** $D = 5 \cdot 10^{-21}$, **c** $D = 5 \cdot 10^{-11}$, **d** $D = 5 \cdot 10^{-3}$. Color code: 1-cluster chimera death (1-CD), 3-cluster chimera death (3-CD), multi-cluster chimera death (n -CD, $n > 3$), in-phase synchronized oscillations and coherent traveling waves (SYNC). Initial condition: Snapshot of an amplitude chimera calculated for $D = 0$, $P = 4$, $\sigma = 14$, $t = 150$. Maximum simulation time: $t = 5000$. Parameters: $N = 100$, $\lambda = 1$, $\omega = 2$

states, either in-phase synchronized oscillations or traveling waves (dark blue region, labeled SYNC). For very small coupling range, we observe amplitude chimeras as transients. For larger σ and P , we find chimera death states (yellow, orange, and red regions) with one coherent domain (1-CD), or for slightly smaller P , with three (3-CD), or more (n -CD with $n > 3$) coherent domains. For all noise intensities, there exists a chimera death regime (1-CD, 3-CD, n -CD), as well as a coherent oscillatory regime (SYNC).

The regime of chimera death states is characterized by high multistability. The boundary between the oscillatory regime and the chimera death regime is roughly independent of the particular amplitude chimera snapshot used as initial condition. In contrast, for many values of (σ, P) , the particular type of chimera death depends on the realization of the initial condition. Note that there is nevertheless a clear tendency that the m -CD patterns (with $m < k$) are generally found for larger coupling ranges than the k -CD states ($k, m \in \{1, 3, n\}$). This tendency is especially pronounced for large coupling strengths. Noise influences the dynamic regimes in different ways. First, the boundaries between the different cluster types of chimera death appear to be almost unaffected by the applied external noise. We do not observe any noise-induced switching between the different types of chimera death. The applied noise does not influence the asymptotic chimera death state. Second, with increasing noise intensity, the boundary between the oscillatory regime and the oscillation death regime is shifted towards higher coupling strengths. This means that the stochastic force pushes the system out of the deterministic inhomogeneous steady state into the basin of attraction of the stable coherent oscillatory state, and induces oscillations in a parameter regime where in the absence of noise the steady state is a stable asymptotic solution. The size of this parameter regime depends on the applied noise intensity. In order to facilitate the comparison, the boundaries between the oscillatory regime and the chimera death regime are depicted for different noise intensities in Fig. 1.12.

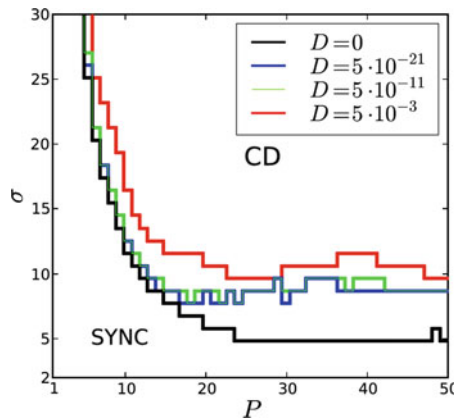


Fig. 1.12 Boundary between the oscillatory regime and the chimera death regime for different noise intensities D , extracted from the maps of dynamic regimes shown in Fig. 1.11

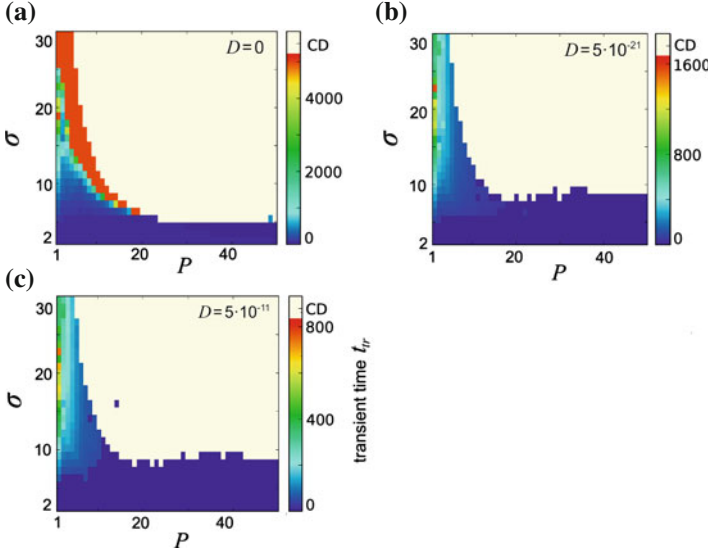


Fig. 1.13 Transient times of amplitude chimeras t_{tr} in the plane of coupling strength σ and number of nearest neighbors P , for the noise intensities: **a** $D = 0$, **b** $D = 5 \cdot 10^{-21}$, **c** $D = 5 \cdot 10^{-11}$. System parameters, initial condition and simulation time as in Fig. 1.11

Generally, the stronger the applied noise is, the smaller is the regime of chimera death states.

In the oscillatory regime, we observe transient amplitude chimeras. In Fig. 1.13 their lifetimes are depicted, obtained from the same simulations described above. One can see that generally the transient time decreases with decreasing coupling strength, and with increasing noise intensity, as shown already in Figs. 1.8 and 1.9 for a restricted range of coupling parameters. Note that Fig. 1.13b ($D = 5 \cdot 10^{-11}$) and Fig. 1.13c ($D = 5 \cdot 10^{-21}$) look very similar up to rescaling of the transient times. This illustrates that the impact of the applied noise upon the dynamics is rather independent of the strength and range of the coupling.

In the deterministic case (Fig. 1.13a) there is a regime of high values of the coupling strength, at the border between the oscillatory regime and the chimera death regime, where the transient amplitude chimeras last longer than the maximum simulation time of $t = 5000$ (bright orange). For several values of (σ, P) in this region, we have simulated much longer time series until $t = 40,000$ (more than 12,700 oscillation periods T), and have found that the amplitude chimeras persist. However, they disappear much earlier as soon as a tiny amount of external noise is applied. This indicates that the amplitude chimera states are also unstable in this region. The extremely long transient times might simply be related to our choice of initial conditions in the deterministic system.

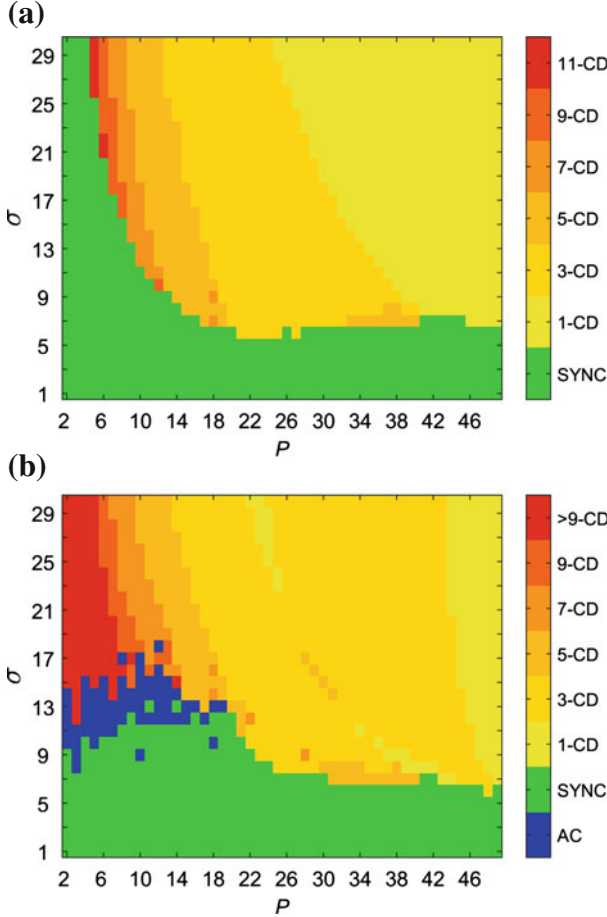


Fig. 1.14 Map of dynamic regimes in the plane of number of nearest neighbors P and coupling strength σ **a** for $\tau = 0$ and **b** $\tau = \pi$. Color scale: 1-CD 1-cluster chimera death; 3-CD 3-cluster chimera death; n -CD n -cluster chimera death. SYNC coherent states (synchronized oscillations, traveling waves). AC amplitude chimera. Parameters: $N = 100$, $\lambda = 1$, $\omega = 2$

1.6 Control of Chimeras by Time Delay

We have shown that amplitude chimeras are preserved in the stochastic case and their lifetime can be decreased by tuning the noise intensity. Next we demonstrate that amplitude chimeras are also observed for the time-delayed coupling and their lifetime can be significantly enlarged by an appropriate choice of delay time.

As initial condition for the simulation of the system Eq. (1.3) we choose a snapshot of an amplitude chimera. The corresponding phase diagram for $\tau = 0$ is illustrated in Fig. 1.14a. Since the integration time used for this plot is rather large ($t = 5000$),

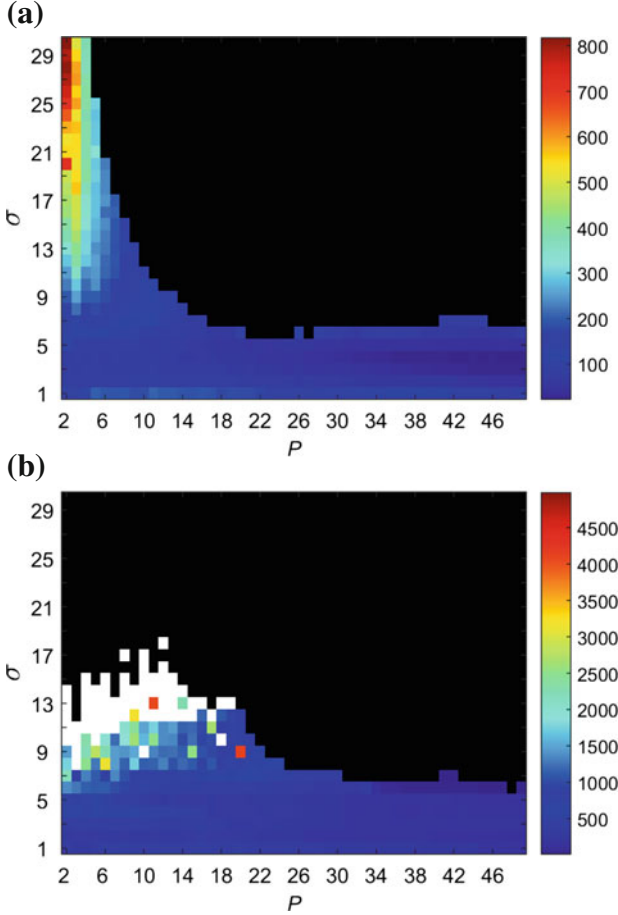
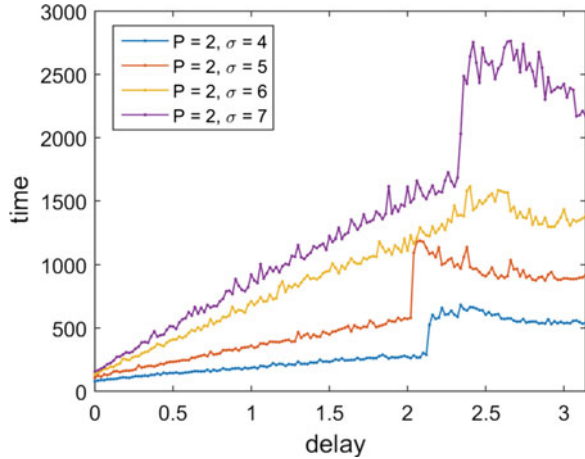


Fig. 1.15 Transient times t_{tr} in the plane of number of nearest neighbors P and coupling strength σ : color code indicates the time of transition from incoherent states (amplitude chimera) to coherent states for **a** $\tau = 0$ and **b** $\tau = \pi$. The black region marks chimera death states. Integration time until $t = 5000$. The white dots are amplitude chimeras and related structures that are stable in the simulation timespan. Parameters: $\lambda = 1$, $\omega = 2$, $N = 100$

amplitude chimeras do not survive for that long in the absence of time-delayed coupling and transform into the in-phase synchronized regime (green region in Fig. 1.14a). Therefore, for $\tau = 0$ the phase diagram contains only chimera death states with different number of clusters and asymptotic coherent states (in-phase synchronized oscillations and coherent travelling waves).

In the presence of delay, however, amplitude chimeras live significantly longer. In particular, for $\tau = \pi$, which corresponds to the period of the single Stuart-Landau oscillator, they still exist at $t = 5000$ for a certain range of coupling strength $7 < \sigma < 19$ and number of nearest neighbors $2 < P < 20$, see Fig. 1.14b. Moreover, chimera

Fig. 1.16 Transient times t_{tr} of amplitude chimeras in dependence on time delay τ for different values of coupling strength $\sigma = 4, 5, 6, 7$. Other parameters: $N = 100$, $\omega = 2$, $\lambda = 1$, $P = 2$



death patterns with large number of clusters now dominate while the region of 1-cluster chimera death is strongly reduced. Additionally, the in-phase synchronized state observed in the deterministic system for small number of nearest neighbors ($P < 6$) and large coupling strength ($\sigma > 15$) in the presence of time delay is replaced by chimera death patterns with the number of clusters exceeding 9 (red region in Fig. 1.14b).

To compare directly the results for the lifetime of amplitude chimeras we calculate transient times t_{tr} in the plane of number of nearest neighbors P and coupling strength σ for $\tau = 0$ and $\tau = \pi$ (Fig. 1.15a, b, respectively). In both cases chimera death states are the dominating patterns in the phase diagram (black color in Fig. 1.15). The long-living amplitude chimeras ($t_{tr} \geq 5000$) appear only when the links between the nodes include time delay (white region in Fig. 1.15b), while for $\tau = 0$ the lifetime of amplitude chimera is relatively short ($t_{tr} < 900$).

In order to quantitatively characterize the impact of the time-delayed coupling we calculate the lifetime of amplitude chimeras in dependence on time delay for different values of coupling strength $\sigma = 4, 5, 6, 7$ (Fig. 1.16). The transient times increase with time delay for all considered values of σ . Therefore, by appropriately choosing the value of time delay one can realize a desired lifetime of amplitude chimeras.

1.7 Conclusions

We have investigated two types of chimera states for a paradigmatic network of oscillators under the influence of noise and time delay. We have presented numerical results demonstrating that transient amplitude chimeras and chimera death states in a ring network of identical Stuart-Landau oscillators with symmetry-breaking

coupling continue to exist in the presence of Gaussian white noise or if time delay is introduced to the coupling.

In the presence of external noise, transient amplitude chimeras occur in the same range of coupling parameters as in the deterministic case. The key quantity we use to characterize them is the transient time. The latter decreases logarithmically with the applied noise intensity. For a constant noise intensity, the transient times increase with the coupling strength up to a saturation value. The amplitude chimera lifetimes depend sensitively on the particular realization of the randomized initial condition. We have introduced a class of specially prepared random initial conditions that produce long lasting amplitude chimeras. We have shown that initial configurations that fulfill a symmetry conditions which is also found in oscillation death patterns result in the longest living amplitude chimera transients.

The chimera death patterns also persist under the impact of stochastic forces. However, the coupling parameter regime where they occur is reduced with increasing noise intensity. The boundary between the coherent oscillatory regime and the chimera death regime is shifted towards higher values of the coupling strength. That means that the system favors oscillatory behavior for a larger coupling parameter regime. In contrast, this boundary appears to be independent on the particular realization of the initial condition. The number of clusters within the coherent domains appears to be unaffected by the external noise, but depends on the particular initial condition.

In the presence of time delay the lifetime of amplitude chimera patterns is essentially enlarged. Moreover, time delay induces amplitude chimeras for the coupling parameter values for which in the absence of time delay no chimera patterns are observed.

Thus, the lifetime of amplitude chimeras can be controlled by tuning the noise intensity and the value of time delay, which, therefore, play the role of control parameters. Noise allows one to decrease the lifetime of amplitude chimeras, while time delay can significantly increases it.

Our numerical findings can be explained by the underlying phase space structure. More specifically, we propose that amplitude chimera states can be represented by saddle states in the phase space of the network. This elucidates the behavior of their lifetime, and explains that generally the initial conditions become less important under the influence of noise.

Acknowledgments This work was supported by DFG in the framework of SFB 910.

References

1. M.J. Panaggio, D.M. Abrams, Chimera states: Coexistence of coherence and incoherence in networks of coupled oscillators. *Nonlinearity* **28**, R67 (2015)
2. Y. Kuramoto, D. Battogtokh, Coexistence of coherence and incoherence in nonlocally coupled phase oscillators. *Nonlin. Phen. in Complex Sys.* **5**(4), 380–385 (2002)
3. D.M. Abrams, S.H. Strogatz, Chimera states for coupled oscillators. *Phys. Rev. Lett.* **93**(17), 174102 (2004)

4. D.M. Abrams, R.E. Mirollo, S.H. Strogatz, D.A. Wiley, Solvable model for chimera states of coupled oscillators. *Phys. Rev. Lett.* **101**(8), 084103 (2008)
5. G.C. Sethia, A. Sen, F.M. Atay, Clustered chimera states in delay-coupled oscillator systems. *Phys. Rev. Lett.* **100**(14), 144102 (2008)
6. C.R. Laing, The dynamics of chimera states in heterogeneous Kuramoto networks. *Physica D* **238**(16), 1569–1588 (2009)
7. A.E. Motter, Nonlinear dynamics: spontaneous synchrony breaking. *Nat. Phys.* **6**(3), 164–165 (2010)
8. E.A. Martens, C.R. Laing, S.H. Strogatz, Solvable model of spiral wave chimeras. *Phys. Rev. Lett.* **104**(4), 044101 (2010)
9. S. Olmi, A. Politi, A. Torcini, Collective chaos in pulse-coupled neural networks. *Europhys. Lett.* **92**, 60007 (2010)
10. G. Bordyugov, A. Pikovsky, M. Rosenblum, Self-emerging and turbulent chimeras in oscillator chains. *Phys. Rev. E* **82**(3), 035205 (2010)
11. J.H. Sheeba, V.K. Chandrasekar, M. Lakshmanan, Chimera and globally clustered chimera: impact of time delay. *Phys. Rev. E* **81**, 046203 (2010)
12. A. Sen, R. Dodla, G. Johnston, G.C. Sethia, Amplitude death, synchrony, and chimera states in delay coupled limit cycle oscillators, in *Complex Time-Delay Systems*, vol. 16, Understanding Complex Systems, ed. by F.M. Atay (Springer, Berlin, 2010), pp. 1–43
13. M. Wolfrum, O.E. Omel'chenko, Chimera states are chaotic transients. *Phys. Rev. E* **84**(1), 015201 (2011)
14. C.R. Laing, Fronts and bumps in spatially extended Kuramoto networks. *Phys. D* **240**(24), 1960–1971 (2011)
15. I. Omelchenko, Y. Maistrenko, P. Hövel, E. Schöll, Loss of coherence in dynamical networks: spatial chaos and chimera states. *Phys. Rev. Lett.* **106**, 234102 (2011)
16. I. Omelchenko, B. Riemenschneider, P. Hövel, Y. Maistrenko, E. Schöll, Transition from spatial coherence to incoherence in coupled chaotic systems. *Phys. Rev. E* **85**, 026212 (2012)
17. I. Omelchenko, O.E. Omel'chenko, P. Hövel, E. Schöll, When nonlocal coupling between oscillators becomes stronger: patched synchrony or multichimera states. *Phys. Rev. Lett.* **110**, 224101 (2013)
18. S. Nkomo, M.R. Tinsley, K. Showalter, Chimera states in populations of nonlocally coupled chemical oscillators. *Phys. Rev. Lett.* **110**, 244102 (2013)
19. J. Hizanidis, V. Kanas, A. Bezerianos, T. Bountis, Chimera states in networks of nonlocally coupled hindmarsh-rose neuron models. *Int. J. Bifurcat. Chaos* **24**(03), 1450030 (2014)
20. G.C. Sethia, A. Sen, G.L. Johnston, Amplitude-mediated chimera states. *Phys. Rev. E* **88**(4), 042917 (2013)
21. G.C. Sethia, A. Sen, Chimera states: the existence criteria revisited. *Phys. Rev. Lett.* **112**, 144101 (2014)
22. A. Yeldesbay, A. Pikovsky, M. Rosenblum, Chimeralike states in an ensemble of globally coupled oscillators. *Phys. Rev. Lett.* **112**, 144103 (2014)
23. F. Böhm, A. Zakharova, E. Schöll, K. Lüdge, Amplitude-phase coupling drives chimera states in globally coupled laser networks. *Phys. Rev. E* **91**(4):040901 (R) (2015)
24. A. Buscarino, M. Frasca, L.V. Gambuzza, P. Hövel, Chimera states in time-varying complex networks. *Phys. Rev. E* **91**(2), 022817 (2015)
25. I. Omelchenko, A. Provata, J. Hizanidis, E. Schöll, P. Hövel, Robustness of chimera states for coupled FitzHugh-Nagumo oscillators. *Phys. Rev. E* **91**, 022917 (2015)
26. I. Omelchenko, A. Zakharova, P. Hövel, J. Siebert, E. Schöll, Nonlinearity of local dynamics promotes multi-chimeras. *Chaos* **25**, 083104 (2015)
27. P. Ashwin, O. Burylko, Weak chimeras in minimal networks of coupled phase oscillators. *Chaos* **25**, 013106 (2015)
28. V. Bastidas, I. Omelchenko, A. Zakharova, E. Schöll, T. Brandes, Quantum signatures of chimera states. *Phys. Rev. E* **92**, 062924 (2015)
29. N. Semenova, A. Zakharova, E. Schöll, V.S. Anishchenko, Does hyperbolicity impede emergence of chimera states in networks of nonlocally coupled chaotic oscillators? *Europhys. Lett.* **112**, 40002 (2015)

30. A.M. Hagerstrom, T.E. Murphy, R. Roy, P. Hövel, I. Omelchenko, E. Schöll, Experimental observation of chimeras in coupled-map lattices. *Nat. Phys.* **8**, 658–661 (2012)
31. M.R. Tinsley, S. Nkomo, K. Showalter, Chimera and phase cluster states in populations of coupled chemical oscillators. *Nat. Phys.* **8**, 662–665 (2012)
32. E.A. Martens, S. Thutupalli, A. Fourriere, O. Hallatschek, Chimera states in mechanical oscillator networks. *Proc. Nat. Acad. Sci.* **110**, 10563 (2013)
33. L. Larger, B. Penkovsky, Y. Maistrenko, Virtual chimera states for delayed-feedback systems. *Phys. Rev. Lett.* **111**, 054103 (2013)
34. T. Kapitaniak, P. Kuzma, J. Wojewoda, K. Czołczynski, Y. Maistrenko, Imperfect chimera states for coupled pendula. *Sci. Rep.* **4**, 6379 (2014)
35. M. Wickramasinghe, I.Z. Kiss, Spatially organized dynamical states in chemical oscillator networks: synchronization, dynamical differentiation, and chimera patterns. *PLoS ONE* **8**(11), e80586 (2013)
36. M. Wickramasinghe, I.Z. Kiss, Spatially organized partial synchronization through the chimera mechanism in a network of electrochemical reactions. *Phys. Chem. Chem. Phys.* **16**, 18360–18369 (2014)
37. L. Schmidt, K. Schönleber, K. Krischer, V. Garcia-Morales, Coexistence of synchrony and incoherence in oscillatory media under nonlinear global coupling. *Chaos* **24**(1), 013102 (2014)
38. L.V. Gambuzza, A. Buscarino, S. Chessa, L. Fortuna, R. Meucci, M. Frasca, Experimental investigation of chimera states with quiescent and synchronous domains in coupled electronic oscillators. *Phys. Rev. E* **90**, 032905 (2014)
39. D.P. Rosin, D. Rontani, N.D. Haynes, E. Schöll, D.J. Gauthier, Transient scaling and resurgence of chimera states in coupled Boolean phase oscillators. *Phys. Rev. E* **90**, 030902(R) (2014)
40. L. Larger, B. Penkovsky, Y. Maistrenko, Laser chimeras as a paradigm for multistable patterns in complex systems. *Nat. Comm.* **6**, 7752 (2015)
41. C.R. Laing, C.C. Chow, Stationary bumps in networks of spiking neurons. *Neural Comput.* **13**(7), 1473–1494 (2001)
42. J.M. Davidenko, A.M. Pertsov, R. Salomonsz, W. Baxter, J. Jalife, Stationary and drifting spiral waves of excitation in isolated cardiac muscle. *Nature* **355**, 349 (1992)
43. A.E. Motter, S.A. Myers, M. Anghel, T. Nishikawa, Spontaneous synchrony in power-grid networks. *Nat. Phys.* **9**, 191–197 (2013)
44. J.C. Gonzalez-Avella, M.G. Cosenza, M.S. Miguel, Localized coherence in two interacting populations of social agents. *Phys. A* **399**, 24–30 (2014)
45. N.C. Rattenborg, C.J. Amlaner, S.L. Lima, Behavioral, neurophysiological and evolutionary perspectives on unihemispheric sleep. *Neurosci. Biobehav. Rev.* **24**, 817–842 (2000)
46. A. Rothkegel, K. Lehnertz, Irregular macroscopic dynamics due to chimera states in small-world networks of pulse-coupled oscillators. *New J. Phys.* **16**, 055006 (2014)
47. A. Zakharova, M. Kapeller, E. Schöll, Chimera death: symmetry breaking in dynamical networks. *Phys. Rev. Lett.* **112**, 154101 (2014)
48. F.M. Atay, Distributed delays facilitate amplitude death of coupled oscillators. *Phys. Rev. Lett.* **91**, 094101 (2003)
49. A. Zakharova, I. Schneider, Y.N. Kyrychko, K.B. Blyuss, A. Koseska, B. Fiedler, E. Schöll, Time delay control of symmetry-breaking primary and secondary oscillation death. *Europhys. Lett.* **104**, 50004 (2013)
50. A. Zakharova, M. Kapeller, E. Schöll, Amplitude chimeras and chimera death in dynamical networks. *J. Phys. Conf. Ser.* (2015). [arXiv:1503.03371](https://arxiv.org/abs/1503.03371)
51. H. Risken, *The Fokker-Planck Equation*, 2nd edn. (Springer, Berlin, 1996)
52. I. Schneider, M. Kapeller, S. Loos, A. Zakharova, B. Fiedler, E. Schöll, Stable and transient multi-cluster oscillation death in nonlocally coupled networks. *Phys. Rev. E* **92**, 052915 (2015)
53. T. Banerjee, Mean-field diffusion-induced chimera death state. *Europhys. Lett.* **110**, 60003 (2015)
54. S. Loos, A. Zakharova, J.C. Claussen, E. Schöll, Chimera patterns under the impact of noise. *Phys. Rev. E* (2016). [arXiv:1508.04010v2](https://arxiv.org/abs/1508.04010v2)

<http://www.springer.com/978-3-319-28027-1>

Control of Self-Organizing Nonlinear Systems

Schöll, E.; Klapp, S.H.L.; Hövel, P. (Eds.)

2016, XVII, 475 p. 159 illus., 117 illus. in color.,

Hardcover

ISBN: 978-3-319-28027-1